THE JOURNAL OF PHYSICAL CHEMISTRY B

B: Biomaterials and Membranes

Perturbation of Hydrogen Bonding Networks Over Supported Lipid Bilayers by Poly (allylamine hydrochloride)

Naomi Dalchand, Merve Do#angün, Paul E Ohno, Emily Ma, Alex B. F. Martinson, and Franz M. Geiger

J. Phys. Chem. B, **Just Accepted Manuscript** • DOI: 10.1021/acs.jpcb.9b02392 • Publication Date (Web): 23 Apr 2019

ACS Publications

is published by the American Chemical Society. 1155 Sixteenth Street N.W., Washington, DC 20036

Perturbation of Hydrogen Bonding Networks Over Supported Lipid Bilayers by Poly (allylamine hydrochloride)

Naomi Dalchand,[a] Merve Doğangün,[a] Paul E. Ohno,[a] Emily Ma,[a] Alex B. F. Martinson,[b] and Franz M. Geiger [a]*

[a]Department of Chemistry, Northwestern University, 2145 Sheridan Road, Evanston, IL 60660

[b]Materials Science Division, Argonne National Lab, 9700 S Cass Ave., Argonne IL 40439

*Corresponding Author. Email: geigerf@chem.northwestern.edu.

ABSTRACT. Water is vital to many biochemical processes and is necessary for driving many fundamental interactions of cell membranes with their external environments, yet it is difficult to probe the membrane/water interface directly and without the use of external labels. Here, we employ vibrational sum frequency generation (SFG) spectroscopy to understand the role of interfacial water molecules above bilayers formed from zwitterionic (phosphatidylcholine, PC) and anionic (phosphatidylglycerol, PG, and phosphatidylserine, PS) lipids as they are exposed to the common polycation poly (allylamine hydrochloride) (PAH) in 100 mM NaCl. We show that as the concentration of PAH is increased, the interfacial water molecules are irreversibly displaced and find that it requires 10 times more PAH to displace interfacial water molecules from membranes formed from purely zwitterionic lipids when compared to membranes that contain the anionic PG and PS lipids. This outcome is likely due to difference in (1) the energy with which water molecules are bound to the lipid headgroups, (2) the number of water molecules bound to the headgroups, which is related to the headgroup area, and (3) the electrostatic interactions between the PAH molecules and the negatively charged lipids that are favored when compared to

the zwitterionic lipid headgroups. The findings presented here contribute to establishing causal relationships in nanotoxicology and to understanding, controlling, and predicting the initial steps that lead to the lysis of cells exposed to membrane disrupting polycations, or to transfection.

I. Introduction. Cell membranes act as selective barriers to control the movement of ions and small molecules into and out of the cell.[1,2] This function is important in maintaining a homeostatic aqueous environment on both sides of the membrane, where vital biochemical processes occur.[3-5] Therefore, unanticipated changes to cell membranes can also alter their surrounding environment, ultimately disrupting important biological pathways. It has been reported that ions, polycations, and nanomaterials are prone to perturb supported lipid bilayers (SLBs), idealized model cell membranes,[3,6] and cause physical changes such as lipid asymmetry[7-10] and the formation of lipid coronas.[11-14] While informative, these results are specific to the SLBs and not their surrounding aqueous environment. Thus, further analysis of the aqueous surroundings is an important factor in obtaining a complete and fundamental understanding of the molecular mechanisms associated with membrane interactions. To this end, we focus on the water above SLBs due to its ubiquitous presence in biochemical environments.[15,16] Moreover, water at biologically relevant membranes exhibit properties that are still under debate, including those influencing structural networks resembling ice vs water[1,17] or bulk-like vs considerably reduced relative permittivity.[18]

Here, we monitor the interfacial hydrogen-bonding (H-bonding) network above membranes formed from zwitterionic and anionic lipids as we add varying concentrations of the cationic polymer poly (allylamine hydrochloride) (PAH, Fig. 1A). PAH is widely used as a coating for nanoparticles[19-21] and exists in substantial amounts as free PAH in equilibrium with bound PAH in nanoparticle solutions, even after purification. Given the toxicity of PAH to bacteria,[22] it is of interest to analyze free PAH with lipid membranes so as to further understand its lysing action.

While our prior studies of free-PAH characterized the thermodynamic and structural changes to SLBs upon PAH adsorption by monitoring structural changes to the lipids in the C−H stretching region,[11,23] we now focus specifically on probing how the H-bond network of the water molecules that constitute the electrical double layer over the membrane varies during interaction with the polycations. Given their importance in biological membranes, we study lipids terminated with the zwitterionic phosphocholine (PC) headgroup as well as the anionic phospho-(1-*rac*-glycerol) and phospho-L-serine (PG and PS) headgroups (Fig. 1B-1D).

To probe the very initial stages of membrane disruption by PAH, which presumably involves PAH interactions with the membrane-bound water molecules, we employ μM polycation concentrations but also employ higher polycation concentrations, which disrupt the bilayers permanently, as demonstrated in detail in our prior work.[11] We now probe the water O−H stretching region and do so with vibrational sum frequency generation (SFG) spectroscopy. This technique is a naturally appropriate for studying aqueous interfaces, as it is inherently surface sensitive,[16,24,25-28] allowing us to probe a thin interfacial region of water above the membrane while providing detailed molecular information about the strength of the hydrogen bond network through a detailed analysis of the second-order spectral lineshapes.[29-31] Prior work has shown that the membrane/water interface is a challenge to probe directly using SFG spectroscopy due to the symmetric constraints that govern the sum frequency process. To offset these constraints, past studies have employed asymmetric, chemically modified bilayers by deuteration of one of the bilayer leaflets. Our recent work using a commercially available broadband laser system at kHz repetition rates has shown to overcome these restrictions and provide spectra with relatively good S/N after short acquisition times for unlabeled, symmetric bilayers.[36]

We find evidence for the displacement of interfacial water molecules for lipid bilayers formed from zwitterionic and negatively charged lipids in a fashion that impacts both strong and weak H-bond interactions. Rinsing does not lead to SFG signal recovery from the C−H and O−H oscillators, indicating that the irreversibility of PAH interaction with membranes rich in lipids such as those studied here may be detrimental to membrane function and cellular integrity. As PAH attachment blocks solvated ions and water molecules at the membrane surface, irregular diffusion and cell lysis is expected.[32, 33]

II. Methods. Unless indicated otherwise, we follow our previously published methods.[8-9,11,19,23,34] The sections below briefly summarize the approach for the reader's convenience.

IIA. Polymer and Vesicle Preparation. Poly (allylamine hydrochloride) (PAH, 17.5 kDa) was purchased from Sigma-Aldrich and used without further purification. All stock solutions of PAH were made and stored in 0.001 M NaCl. These solutions were then diluted with buffer composed of 0.01 M Tris and 0.1 M NaCl to the final PAH concentrations used for the experiments shown in sections III.A. - III.C. The buffer was corrected to a final pH of 7.40 ± 0.05 with NaOH and HCl.

The lipids 1,2-Dimyristoyl-*sn*-glycero-3-phosphocholine (DMPC), 1,2-dimyristoyl-*sn*-glycero-3-phospho-(1-*rac*-glycerol) (DMPG), and 1,2-dimyristoyl-*sn*-glycero-3-phospho-L-serine (DMPS) were purchased from Avanti Polar Lipids. Small unilamellar vesicles were prepared from 2 mg suspensions of the following lipid combinations: 100 mol % DMPC, 90 mol % DMPC and 10 mol % DMPG, and 90 mol % DMPC and 10 mol % DMPS. The vesicle solutions were dried with N_2 and left in the desiccator overnight to remove any excess chloroform. The dried vesicle films were then resuspended in 0.01 M Tris and 0.1 M NaCl buffer containing 0.005 M $CaCl_2$ and extruded using a mini-extruder kit as we have shown previously.[35,36] SLBs are then formed using the vesicle fusion method[37,38] on 3 mm CaF_2 windows (ISP-Optics) coated with 25 nm of SiO_2 by atomic layer deposition (ALD). Calcium-free 0.01 M Tris and 0.1 M NaCl buffer (pH 7.4) was used for bilayer formation. Our SLBs have previously been well characterized.[26]

IIB. Substrate Preparation with Atomic Layer Deposition (ALD). To avoid spurious optical contributions to the detected SFG signal from color centers that are present to varying extent within commercially available fused silica windows, we coated CaF_2 windows, which are free of such center, with a thin ALD silica overlayer processed in a 125°C reactor under Argon flow in which 3DMAS [Tris (dimethylamino) silane] was added for 0.4 s, followed by a 10 s purge. O_2 plasma was then introduced for 20 s, followed by a 12 s purge. To yield a SiO_2 film of 25 nm thickness, this process was repeated for ~300 cycles. The final thickness of SiO_2 on the CaF_2 windows was then estimated from modeling the thickness deposited on witness Si substrates with variable angle spectroscopic ellipsometry.[39] For clarity, these windows will be referred to as 25 nm ALD SiO_2 substrates.

IIC. Vibrational Sum Frequency Generation Spectroscopy. SFG experiments were conducted using a Ti:Sapphire laser system (Solstice, Spectra Physics, 795 nm, 3 mJ/pulse, 1 kHz repetition rate, 120 fs pulse duration). Details of our experimental set-up have been previously reported.[34] Briefly, we monitored changes in the C−H (2800-3000 cm^{-1}) and O−H (3000 cm^{-1}-3600 cm^{-1}) stretching regions. All experiments were carried out in triplicate and conducted using internal reflection geometry. Multiple individual spectra were taken at different center IR wavelengths and different detector positions prior to being compiled together following the procedure discussed in our previous work.[34] All spectra were taken in *ssp*-polarization (*s*-polarized SFG, *s*-polarized 800 nm light, and *p*-polarized IR light) and normalized to spectra from gold coated on a CaF_2 window in *ppp*-polarization to account for the IR spectral profile (see Supporting Information Figure S1).

IID. PAH-Membrane Interaction Experiments. Following bilayer formation, PAH was introduced into a home-built Teflon flow-cell at a starting concentration of 1 μM. Two acquisitions were taken in the frequency range of interest, 2800-3600 cm^{-1}, before the next concentration was introduced and averaged to produce a representative spectrum for each concentration. PAH addition was stopped after the SLBs had undergone substantial perturbation. After the highest concentration of PAH was introduced, the SLBs were rinsed with 20 mL of PAH-free buffer in order to determine if changes to the SLBs are reversible.

III. Results and Discussion.

IIIA. PAH Displaces Interfacial Water from Negatively Charged Membranes. Figure 2A shows the *ssp*-polarized spectrum of a SLB formed from a mixture of 9:1 DMPC:DMPG lipids exposed to varying PAH concentrations. Our prior work shows the PAH surface coverage for a bilayer formed from a 9:1 mix of DMPC:DMPG to be dense, consistent with monolayer limit.[23] PAH attaches to the membrane through electrostatic interactions and not only changes the surface charge and the lipid order[23,40-44] but is shown here to also displace the interfacial water molecules. In the C−H stretching region, Figure 2A shows what we had reported earlier for the C−H stretching region, namely peaks at ~2880 cm^{-1}, ~2900 cm^{-1}, and ~2950 cm^{-1} characteristic of lipids in a well-formed bilayer.[8,9,35] The peak at ~2880 cm^{-1} is attributable to the symmetric CH_3 stretches of the lipid alkyl tails while the SFG intensity of the other two peaks is due to spectral interference from the water molecules, as demonstrated recently using D_2O[35] and spectral lineshape modeling.[27] Adding PAH to the bilayer leads to SFG intensity decreases, indicating a clear perturbation in the lipid structure with the addition of the polycations. Note that our previously reported loss of spectrally resolved peaks in the C−H stretching region at 1 μM PAH[11] is somewhat at variance with our current observations, which we attribute to the differences in substrates used for experiments (25 nm ALD SiO_2 on CaF_2 in the present experiments vs. fused SiO_2 in our previous experiments).

In the O−H stretching region, the broad peak centered ~3200 cm^{-1} signifies the presence of strong hydrogen bonds (H-bonds) between water molecules and appears in the frequency region where the O−H stretches of the water molecules in solid ice show their infrared transitions.[45] Earlier dilution work with PC/PG lipids identified SFG signal contributions at ~3100 cm^{-1} to be specific to PC···H_2O interactions.[34] A smaller peak, at ~3400 cm^{-1} is also observed in the spectrum and is attributed to the weakly bonded water molecules above the 9:1 DMPC:DMPG bilayer.[46-48] Figure 2A shows that adding PAH results in a signal intensity decrease across the O−H stretching region probed here. At 0.1 mM PAH this loss is ≥70% of the original SFG signal intensity. As the stronger H-bond network, observed at ~3200 cm^{-1}, is seemingly disrupted by PAH, one may expect an increase in the weaker H-bonding region (~3400 cm^{-1}), however, this is not the case. Instead, the decrease in intensity in the 3200 cm^{-1} and the 3400 cm^{-1} regions suggests a direct displacement of the water molecules by PAH. The same trend is also seen in Figure 2B for another negatively charged bilayer composed of a 9:1 mix of DMPC:DMPS lipids, in which the PS headgroup is less shielded than in PG.

IIIB. Membranes Formed from Zwitterionic Lipids Show Slight Displacement of Interfacial Water. Adding PAH to a bilayer formed from purely zwitterionic DMPC elicits two types of outcomes that fall into a majority category showing little (≤ 30%) to no change to the lipid or water signals upon addition of up to 0.1 mM PAH after which signal intensities drop mainly in the C−H stretching region and to some degree in the O−H stretching region at 1 mM PAH (Figures 3A, observed 4 out of 6 times). These changes in the SFG lineshapes at high PAH concentration are likely due to specific water/ion interactions with the lipids, as controls carried out at 300 mM [salt], which corresponds to the total ionic strength at 1 mM PAH (~160 $–NH_3^+$ repeat units) in 100 mM NaCl is ~300 mM (*vide infra*) (Figure 4D). The minority response (Figure 3B, observed 2 out of 6 times) is characterized by noticeable SFG intensity reduction/elimination in the C−H stretching region at PAH concentrations as low as 10 μM, along with considerable signal reductions around 3200 cm^{-1}, albeit to a lesser extent when compared to the negatively charged bilayers (Figure 2).

We attribute the differences we observe in the PAH-membrane interactions described here to how strongly water molecules are bound to the lipid headgroup and to the strength of the electrostatic PAH-membrane interactions. First, the cationic nature of PAH favors interactions with the overall negatively charged membranes, as is indeed observed here in our majority responses. The carboxylate moiety in the PS headgroup is likely parallel to the other lipids comprising the membrane and is therefore readily accessible to cationic PAH (this is also likely for the PG headgroup due to the condensing effect, described below).[49] Moreover, water is also expected to bind more strongly to the amine and carboxylate groups on PS when compared to the more shielded, less accessible, negatively charged phosphate moiety, where most H-bonding occurs for PC lipids.[50] Regarding the strength with which water molecules are bound to the lipids, we refer to computer simulations by Berkowitz and coworkers[51,52] showing that the area per headgroup is smaller for PS lipids than for PC due to intermolecular H-bonding of the amine and carboxylate moieties (Figure 1B, known as the "condensing effect").[49-50] Intermolecular lipid-lipid interactions are also possible for PG bilayers, in which the glycerol moieties H-bond with the ester carbonyl group, likely decreasing the available area per headgroup and thus the number of bound water molecules.[53,54] Conversely, more water molecules surround PC headgroups than PG or PS.[41]

IIIC. Membrane Water is Irreversibly Displaced by PAH. Rinsing the PAH-exposed membranes with calcium-free buffer showed no signal intensity recovery in the H-bonding network or the C−H oscillators (Figures 4A-C). While irreversibility is only shown for the major response for the pure DMPC bilayer, it was also observed for the minority response (see Supporting Information Figure S8). These results support the notion that the PAH polycations have irreversibly displaced the interfacial water molecules.[43]

Because the ionic strength of 1 mM PAH (0.3 M) is~3x higher than our original buffer solution (0.1 M), a control experiment was carried out to determine whether the changes in the H-bonding network was due to the PAH interaction or ionic strength. Figure 4D shows only negligible changes in the O−H stretching region when the salt concentration is raised from 0.1 to 0.3 M. This outcomes is consistent with negligible absorptive-dispersive mixing between the second-order ($\chi^{(2)}$) and the surface potential-dependent third-order contribution ($\chi^{(3)}\Phi(0)$) to the SFG signal generation process, according to[29-30,34,55-57]

$$\chi^{(2)}_{total} = \chi^{(2)} + cos(\varphi_{DC}) e^{i\varphi_{DC}} \chi^{(3)}\Phi(0) \quad (1)$$

Here, φ_{DC} is the optical phase angle (the "DC phase angle")[57] associated with the electrostatic potential produced by the interfacial charges. For electrical double layer models in which the surface potential decays exponentially into the bulk aqueous phase, $\varphi_{DC}=\arctan(\Delta k_z \lambda_D)$, where Δk_z is the wave veactor mismatch (~1.1×10^7 m^{-1} in our experimental setup) and λ_D is the Debye length in the diffuse layer, which depends on the ionic strength. At >100 mM [salt], φ_{DC} is ~0°.[28] The product $cos(\varphi_{DC}) e^{i\varphi_{DC}}$ then equals +1 and model (1) becomes purely additive in $\chi^{(2)}$ and $\chi^{(3)}\Phi(0)$. Figure 4D is consistent with this model. While we observe no significant change in O−H stretching region as [salt] goes from 0.1 to 0.3 M, we observe an SFG signal intensity decrease in the C−H stretching region, which we attribute to the onset of specific binding of Na^+ to the oxygen atoms in the lipid headgroups at these high salt concentrations, as shown by Cordomi *et al.* at 0.2 M NaCl.[58]

IV. Conclusion. We have shown the perturbation of the H-bonding network of bilayers formed from 100% zwitterionic DMPC as well as from 9:1 mixes of DMPC:DMPG and DMPC:DMPS with the addition of the common cationic polymer PAH in 100 mM NaCl. At 0.1 mM, PAH binds irreversibly to the bilayers that contain the negatively charged PG and PS lipids and displace interfacial water molecules, as revealed by vibrational sum frequency generation spectroscopy. 10 times higher PAH concentrations are required to displace water molecules from the purely zwitterionic bilayer. This outcome is likely due to difference in (1) the energy with which water molecules are bound to the lipid headgroups, (2) the number of water molecules bound to the headgroups, which is related to the headgroup area, and (3) the electrostatic interactions between the PAH molecules and the negatively charged lipids that are favored when compared to the zwitterionic lipid headgroups. The interactions between the polycations and the membranes were further analyzed in reversibility studies that revealed no SFG signal intensity recovery upon rinsing for all PAH-exposed membranes surveyed. The irreversibility of PAH attachment can have significant effects on cell function, as osmosis and membrane diffusion are expected to be altered without access to membrane water molecules or solvated ions. As PAH is continued to be used in nanomaterials and as thin films for biomaterials, it is important to note the toxic outcomes large quantities of PAH can have on biological systems.[17] Taken together, then, it is our hope that our insights will help establishing causal relationships in nanotoxicology, and contribute to understanding, controlling, and predicting the initial steps that lead to the lysis of cells exposed to membrane disrupting polycations.

Supporting Information. Replicate measurements of SFG spectra mentioned throughout this article

Acknowledgements. This work is supported by the National Science Foundation under the Center for Sustainable Nanotechnology, Grant No.CHE-1503408. PEO gratefully acknowledges support from the U.S. National Science Foundation Graduate Research Fellowship Program. PEO also acknowledges support from the Northwestern University Presidential Fellowship. FMG gratefully acknowledges support from a Friedrich Wilhelm Bessel Prize from the Alexander von Humboldt Foundation.

References.

1. Bonn, M.; Bakker, H. J.; Tong, Y.; Backus, E. H. G., No Ice-Like Water at Aqueous Biological Interfaces. *Biointerphases* **2012**, *7*, 20.

2. Nagata, Y.; Mukamel, S., Vibrational Sum-Freuqncy Generation Spectroscopy at the Water/Lipid Interface: Molecular Dynamics Simulation Study. *J. Am. Chem. Soc.* **2010**, *132*, 6434-6442.

3. Chan, Y.-H. M.; Boxer, S. G., Model Membrane Systems and Their Applications. *Curr. Opin. Chem. Biol.* **2007**, *11*, 581-587.

4. Plant, A. L., Supported Hybrid Bilayer Membranes as Rugged Cell Membrane Mimics. *Langmuir* **1999**, *15*, 5128-5135.

5. Tanaka, M.; Sackmann, E., Polymer-Supported Membranes as Models of the Cell Surface. *Nature* **2005**, *437*, 656.

6. Leroueil, P. R.; Berry, S. A.; Duthie, K.; Han, G.; Rotello, V. M.; McNerny, D. Q.; Jr., B., James R.; Orr, B. G.; Banaszak Holl, M. M., Wide Varieties of Cationic Nanoparticles Induce Defects in Supported Lipid Bilayers. *Nano Lett.* **2008**, *8*, 420-424.

7. Brown, K. L.; Conboy, J. C., Electrostatic Induction of Lipid Asymmetry. *J. Am. Chem. Soc.* **2011**, *133*, 8794-8797.

8. Dogangun, M.; Hang, M. N.; Machesky, J.; McGeachy, A. C.; Dalchand, N.; Hamers, R. J.; Geiger, F. M., Evidence for Considerable Metal Cation Concentrations from Lithium Intercalation Compounds in the Nano-Bio Interface Gap. *J. Phys. Chem. C* **2017**, *121*, 27473-27482.

9. Dogangun, M.; Hang, M. N.; Troiano, J. M.; McGeachy, A. C.; Melby, E. S.; Pedersen, J. A.; Hamers, R. J.; Geiger, F. M., Alteration of Membrane Compositional Asymmetry by Licoo2 Nanosheets. *ACS Nano* **2015**, *9*, 8755-8765.

10. Stanglmaier, S.; Hertrich, S.; Fritz, K.; Moulin, J.-F.; Haese-Seiller, M.; Radler, J. O.; Nickel, B., Asymmetric Distribution of Anionic Phopholipids in Supported Lipid Bilayers. *Langmuir* **2012**, *28*, 10818-10821.

11. Olenick, L. L., et al., Lipid Corona Formation from Nanoparticle Interactions with Bilayers. *Chem.* **2018**, *4*, 2709-2723.

12. Bahrami, A. H.; Raatz, M.; Jaime, A.-C.; Michel, R.; Curtis, E. M.; Hall, C. K.; Gradzielski, M.; Lipowsky, R.; Weikl, T. R., Wrapping of Nanoparticles by Membranes. *Adv. Colloid Interface Sci.* **2014**, *208*, 214-224.

13. Zhang, S.; Gao, H.; Bao, G., Physical Principles of Nanoparticle Cellular Endocytosis. *ACS Nano* **2015**, *9*, 8655-8671.

14. Jing, B.; Zhu, Y., Disruption of Supported Lipid Bilayers by Semihydrophobic Nanoparticles *J. Am. Chem. Soc.* **2011**, *133*, 10983-10989.

15. Medders, G. R.; Paesani, F., Dissecting the Molecular Structure of the Air/Water Interface from Quantum Simulations of the Sum-Frequency Generation Spectrum. *J. Am. Chem. Soc.* **2016**, *138*, 3912-3919.

16. Richmond, G. L., Molecular Bonding and Interactions at Aqueous Surfaces as Probed by Vibrational Sum Frequency Spectroscopy. *Chem. Rev.* **2002**, *102*, 2693-724.

17. Livingston, R. A.; Zhang, Z.; Piatkowski, L.; Bakker, H. J.; Hunger, J.; Bonn, M.; Backus, E. H., Water in Contact with a Cationic Lipid Exhibits Bulklike Vibrational Dynamics. *J. Phys. Chem. B* **2016**, *120*, 10069-1008.

18. Schlaich, A.; Knapp, E. W.; Netz, R. R., Water Dielectric Effects in Planar Confinement. *Phys. Rev. Let.* **2016**, *117*, 048001.

19. Troiano, J. M., et al., Direct Probes of 4 Nm Diameter Gold Nanoparticles Interacting with Supported Lipid Bilayers. *J. Phys. Chem. C* **2014**, *119*, 534-546.

20. Silva, T. R.; Brondani, D.; Zapp, E.; Vieira, I. C., Electrochemical Sensor Based on Gold Nanoparticles Stabilized in Poly(Allylamine Hydrochloride) for Determination of Vanillin. *Electroanalysis* **2015**, *27*, 465-472.

21. Buchman, J. T.; Rahnamoun, A.; Landy, K. M.; Zhang, X.; Vartanian, A. M.; Jacob, L. M.; Murphy, C. J.; Hernandez, R.; Haynes, C. L., Using and Environmentally-Relevant Panel of Gram-Negative Bacteria to Access the Toxicity of Polyallylamine Hydrochloride-Wrapped Gold Nanoparticles. *Environ. Sci. Nano* **2018**, *5*, 279-288.

22. Qiu, T. A.; Torelli, M. D.; Vartanian, A. M.; Rackstraw, N. B.; Buchman, J. T.; Jacob, L. M.; Murphy, C. J.; Hamers, R. J.; Haynes, C. L., Quantification of Free Polyelectrolytes Present in Colloidal Suspension, Revealing a Source of Toxic Responses for Polyelectrolyte-Wrapped Gold Nanoparticles. *Anal. Chem.* **2017**, *89*, 1823-1830.

23. Troiano, J. M., et al., Quantifying the Electrostatics of Polycation-Lipid Bilayer Interactions. *J. Am. Chem. Soc.* **2017**, *139*, 5808-5816.

24. Chen, X.; Hua, W.; Huang, Z.; Allen, H. C., Interfacial Water Structure Associated with Phopholipid Membranes Studied by Phase-Sensitive Vibrational Sum Frequency Generation Spectroscopy *J. Am. Chem. Soc.* **2010**, *132*, 11336-11342.

25. Ishiyama, T.; Terada, D.; Morita, A., Hydrogen-Bonding Structure at Zwitterionic Lipid/Water Interface. *J. Phys. Chem. Lett.* **2016**, *7*, 216-220.

26. Mifflin, A. L., et al., Accurate Line Shapes from Sub-1 Cm(-1) Resolution Sum Frequency Generation Vibrational Spectroscopy of Alpha-Pinene at Room Temperature. *Journal of Physical Chemistry A* **2015**, *119*, 1292-1302.

27. Buchbinder, A. M.; Weitz, E.; Geiger, F. M., Pentane, Hexane, Cyclopentane, Cyclohexane, 1-Hexene, 1-Pentene, Cis-2-Pentene, Cyclohexene, and Cyclopentene at Vapor/Alpha-Alumina and Liquid/Alpha-Alumina Interfaces Studied by Broadband Sum Frequency Generation. *The Journal of Physical Chemistry C* **2009**, *114*, 554-566.

28. Stokes, G. Y.; Chen, E. H.; Buchbinder, A. M.; Geiger, F. M., Atmospheric Heterogeneous Stereochemistry. *J. Am. Chem. Soc.* **2009**, *131*, 13733-13737.

29. Ohno, P. E.; Wang, H.; Geiger, F. M., Second-Order Spectral Lineshapes from Charged Interfaces. *Nat. Commun.* **2017**, *8*, 1032.

30. Reddy, S. K.; Thiraux, R.; Wellen Rudd, B. A.; Lin, L.; Adel, T.; Joutsuka, T.; Geiger, F. M.; Allen, H. C.; Morita, A.; Paesani, F., Bulk Contributions Modulate the Sum-Frequency Generation Spectra of Water on Model Sea-Spray Aerosols. *Chem.* **2018**, *4*, 1484-1485.

31. Ohno, P. E.; Wang, H. F.; Paesani, F.; Skinner, J. L.; Geiger, F. M., Second-Order Vibrational Lineshapes from the Air/Water Interface *J. Phys. Chem A* **2018**, *122*, 4457-4464.

32. Fischer, D.; Li, Y.; Ahlemeyer, B.; Krieglstein, J.; Kissel, T., In Vitro Cytotoxicity Testing of Polycations: Influence of Polymer Structure on Cell Viability and Hemolysis. *Biomaterials* **2003**, *24*, 1121-1131.

33. Hong, S.; Leroueil, P. R.; Janus, E. K.; Peters, J. L.; Kober, M.-M.; Islam, M. T.; Orr, B. G.; Jr., B., James R.; Banaszak Holl, M. M., Interaction of Polycationic Polymers with Supported Lipid Bilayers and Cells: Nanoscale Hole Formation and Enhanced Membrane Permeability. *Bioconjugate Chem.* **2006**, *17*, 728-734.

34. Dogangun, M.; Ohno, P. E.; Liang, D.; McGeachy, A. C.; Be, A. G.; Dalchand, N.; Li, T.; Cui, Q.; Geiger, F. M., Hydrogen-Bond Networks near Supported Lipid Bilayers from Vibrational Sum Frequency Generation Experiments and Atomistic Simulations. *J. Phys. Chem. B* **2018**, *122*, 4870-4879.

35. Olenick, L. L.; Chase, H. M.; Fu, L.; Zhang, Y.; McGeachy, A. C.; Dogangun, M.; Walter, S. R.; Wang, H.; Geiger, F. M., Single-Component Supported Lipid Bilayers Probed Using Broadband Nonlinear Optics. *Phys. Chem. Chem. Phys.* **2018**, *20*, 3063-3072.

36. McGeachy, A. C.; Dalchand, N.; Caudill, E. R.; Li, T.; Dogangun, M.; Olenick, L. L.; Chang, H.; Pedersen, J. A.; Geiger, F. M., Interfacial Electrostatics of Poly(Vinylamine Hydrochloride), Poly(Diallyldimethylammonium Chloride), Poly-L-Lysine, and Poly-L-Arginine Interacting with Lipid Bilayers. *Phys. Chem. Chem. Phys.* **2018**, *20*, 10846-10856.

37. Kalb, E.; Frey, S.; Tamm, L. K., Formation of Supported Planar Bilayers by Fusion of Vesicles to Supported Phospholipid Monolayers. *Biochim. Biophys. Acta, Biomembr.* **1992**, *1103*, 307-316.

38. Castellana, E. T.; Cremer, P. S., Solid Supported Lipid Bilayers: From Biophysical Studies to Sensor Design. *Surf. Sci. Rep.* **2006**, *61*, 429-444.

39. Woollam, J. A.; Snyder, P. G., Fundamentals and Applications of Variable Angle Spectroscopic Ellipsometry. *Mat. Sci. Eng., B* **1990**, *5*, 279-283.

40. Kreke, M. R.; Badami, A. S.; Brady, J. B.; Akers, R. M.; Goldstein, A. S., Modulation of Protein Adsorption and Cell Adhesion by Poly(Allylamine Hydrochloride) Heparin Films. *Biomaterials* **2005**, *26*, 2975-2981.

41. Lvov, Y.; Decher, G.; Mohwald, H., Assembly, Structural Characterization, and Thermal Behavior of Layer-by-Layer Deposited Ultrathin Films of Poly(Vinyl Sulfate) and Poly(Allylamine). *Langmuir* **1993**, *9*, 481-486.

42. Decher, G.; Eckle, M.; Schmitt, J.; Struth, B., Layer-by-Layer Assembled Multicomposite Films. *Curr. Opin. Colloid Interface Sci.* **1998**, *3*, 32-39.

43. Kujawa, P.; Audi-Hayet, A.; Selb, J.; Candau, F., Rheological Properties of Multisticker Associative Polyelectrolytes in Semidilute Solutions. *J. Polym. Sci. B* **2004**, *42*, 1640-1655.

44. Jachimska, B.; Jasinski, T.; Warsznski, P.; Adamczyk, Z., Conformations of Poly(Allylamine Hydrochloride) in Electrolyte Solutions: Experimental Measurements and Theoretical Modeling. *Colloids Surf. A* **2010**, *355*, 7-15.

45. Hagen, W.; Tielens, A. G. G. M.; Greenberg, J. M., The Infrared Spectra of Amorphous Solid Water and Ice I, between 10 and 140 K. *Chem. Phys.* **1981**, *56*.

46. Lawrence, C. P.; Skinner, J. L., Ultrafast Infrared Spectroscopy Probes Hydrogen-Bonding Dynamics in Liquid Water. *Chem. Phys. Lett.* **2003**, *369*, 472-477.

47. Shen, Y. R.; Ostroverkhov, V., Sum-Frequency Vibrational Spectroscopy on Water Interfaces: Polar Orientation of Water Molecules at Interfaces. *Chem. Rev.* **2006**, *106*, 1140-1154.

48. Gragson, D. E.; Richmond, G. L., Investigations of the Structure and Hydrogen Bonding of Water Molecules at Liquid Surfaces by Vibrational Sum Frequency Spectroscopy. *J. Phys. Chem. B* **1998**, *102*, 3847-3861.

49. Petrache, H. I.; Tristam-Nagle, S.; Gawrisch, K.; Harries, D.; Parsegian, V. A.; Nagle, J. F., Structure and Fluctuations of Charged Phosphatidylserine Bilayers in the Absense of Salt. *Biophys. J.* **2004**, *86*, 1574-1586.

50. Mondal, J. A.; Nihonyanagi, S.; Yamaguchi, S.; Tahara, T., Three Distinct Water Structures at a Zwitterionic Lipid/Water Interface Revealed by Heterodyne-Detected Vibrational Sum Frequency Generation. *J. Am. Chem. Soc.* **2012**, *134*, 7842-7850.

51. Pandit, S. A.; Berkowitz, M. L., Molecular Dynamics Simulation of Dipalmitoylphosphatidylserine Bilayer with Na+ Counterions. *Biophys. J.* **2002**, *82*, 1818-1827.

52. Bhide, S. Y.; Berkowitz, M. L., Structure and Dynamics of Water at the Interface with Phospholipid Bilayers. *J. Chem. Phys.* **2005**, *123*, 224702.

53. Elmore, D. E., Molecular Dynamics Simulation of a Phosphatidylglyverol Membrane. *FEBS Lett.* **2005**, *580*, 144-148.

54. Murzyn, K.; Zhao, W.; Karttunen, M.; Kurdziel, M.; Rog, T., Dynamics of Water at Membrane Surfaces: Effect of Headgroup Structure. *Biointerphases* **2006**, *1*, 98-105.

55. Boamah, M. D.; Ohno, P. E.; Geiger, F. M.; Eisenthal, K. B., Relative Permittivity in the Electrical Double Layer from Nonlinear Optics. *J. Chem. Phys.* **2019**, *148*, 222808.

56. Ohno, P. E.; Saslow, S. A.; Wang, H.; Geiger, F. M.; Eisenthal, K. B., Phase Referenced Nonlinear Spectroscopy of the Alpha-Quartz/Water Interface. *Nat. Commun.* **2016**, *7*, 13587.

57. Ohno, P. E.; Chang, H.; Spencer, A. P.; Boamah, M. D.; Liu, Y.; Wang, H.-f.; Geiger, F. M., Beyond the Gouy-Chapman Model with Heterodyne-Detected Second Harmonic Generation, arXiv:1903.05707 and chemRxiv.7841177.V1. **2019**.

58. Cordomi, A.; Edholm, O.; Perez, J. J., Effect of Force Field Parameters on Sodium and Potassium Ion Binding to Dipalmitoyl Phosphatidylcholine Bilayers. *J. Chem. Theory Comput.* **2009**, *5*, 2125-2134.

Figure Captions.

Figure 1. The structure of (A) cationic polymer, poly (allylamine) hydrochloride (PAH, blue), (B) zwitterionic lipid, 1,2-dimyristoyl-*sn*-glycero-3-phosphocholine (DMPC, green), (C) negatively charged lipid, 1,2-dimyristoyl-*sn*-glycero-3-phospho-(1-*rac*-glycerol) (DMPG, orange), and (D) negatively charged lipid. 1,2-dimyristoyl-*sn*-glycero-3-phospho-L-serine (DMPS, red).

Figure 2. Representative *ssp*-polarized SFG spectra for a bilayer formed from (A) a 9:1 mixture of DMPC:DMPG lipids (orange) and (B) a 9:1 mixture of DMPC:DMPS lipids (red) in buffer solution composed of 0.01 M Tris and 0.1 M NaCl, adjusted to pH 7.4 before interaction with PAH and after the interaction of the SLB with PAH in increasing concentrations: 1 μM (light blue), 10 μM (blue), and 0.1 mM (dark blue). All spectra in (B) have been binned over three points in *x* and *y* between 3000 cm^{-1} – 3600 cm^{-1} for clearer S/N resolution.

Figure 3. *ssp*-Polarized SFG spectra for (A) major and (B) minor responses for the interaction of PAH with a bilayer formed from 100% DMPC lipids in buffer solution composed of 0.01 M Tris and 0.1 M NaCl, adjusted to pH 7.4 before interaction with PAH (green). The spectra taken after the interaction of the SLB with PAH in increasing concentrations: 1 μM (light blue), 10 μM (blue), 0.1 mM (dark blue), and 1 mM (navy). The spectra for (B) have been binned over three points in *x* and *y* between 3000 cm^{-1} – 3600 cm^{-1} for clearer S/N resolution and comparison with the major response.

Figure 4. Interaction of a bilayer formed from (A) a 9:1 mixture of DMPC:DMPG lipids (orange) and (B) a 9:1 mixture of DMPC:DMPS lipids (red) with the highest concentration of PAH studied, 0.1 mM (dark blue), and after rinsing with 20 mL of PAH-free buffer solution (dotted blue line). The spectra for (B) have been binned over three points in *x* and *y* between 3000 cm^{-1} – 3600 cm^{-1}

for clearer S/N resolution and comparison with other reversibility traces. (C) Interaction of a bilayer formed from 100% DMPC lipids (green) with the highest concentration of PAH studied, 1 mM (navy), and after rinsing with 20 mL of PAH-free buffer solution (dotted blue line). (D) A bilayer formed from 100% DMPC lipids (green) after rinsing with buffer solution composed of 0.01 M Tris and 0.3 M NaCl, adjusted to pH 7.4.

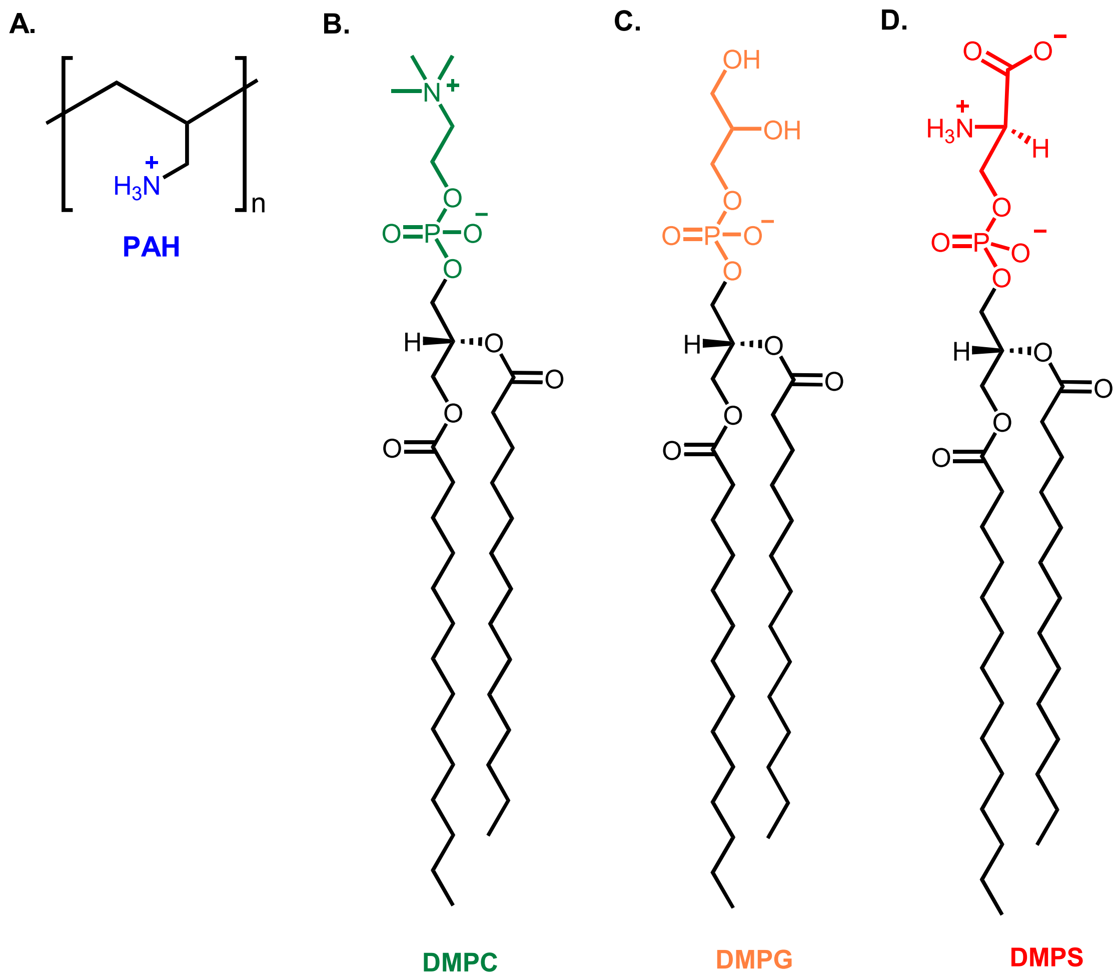

Figure 1.

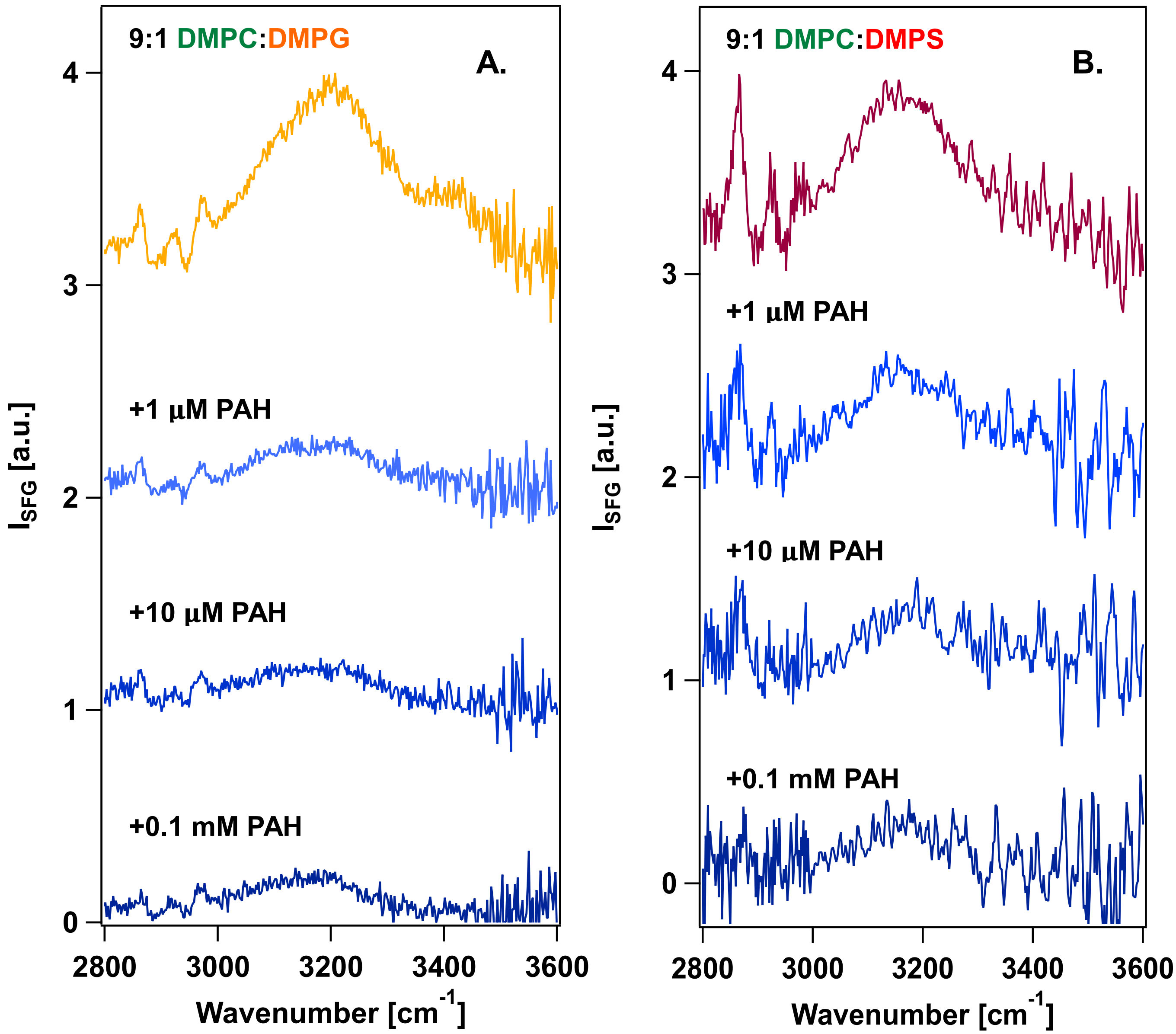
9:1 DMPC:DMPG
A.
+1 µM PAH
+10 µM PAH
+0.1 mM PAH
I_{SFG} [a.u.]
Wavenumber [cm^{-1}]
9:1 DMPC:DMPS
B.
+1 µM PAH
+10 µM PAH
+0.1 mM PAH
I_{SFG} [a.u.]
Wavenumber [cm^{-1}]

Figure 2.

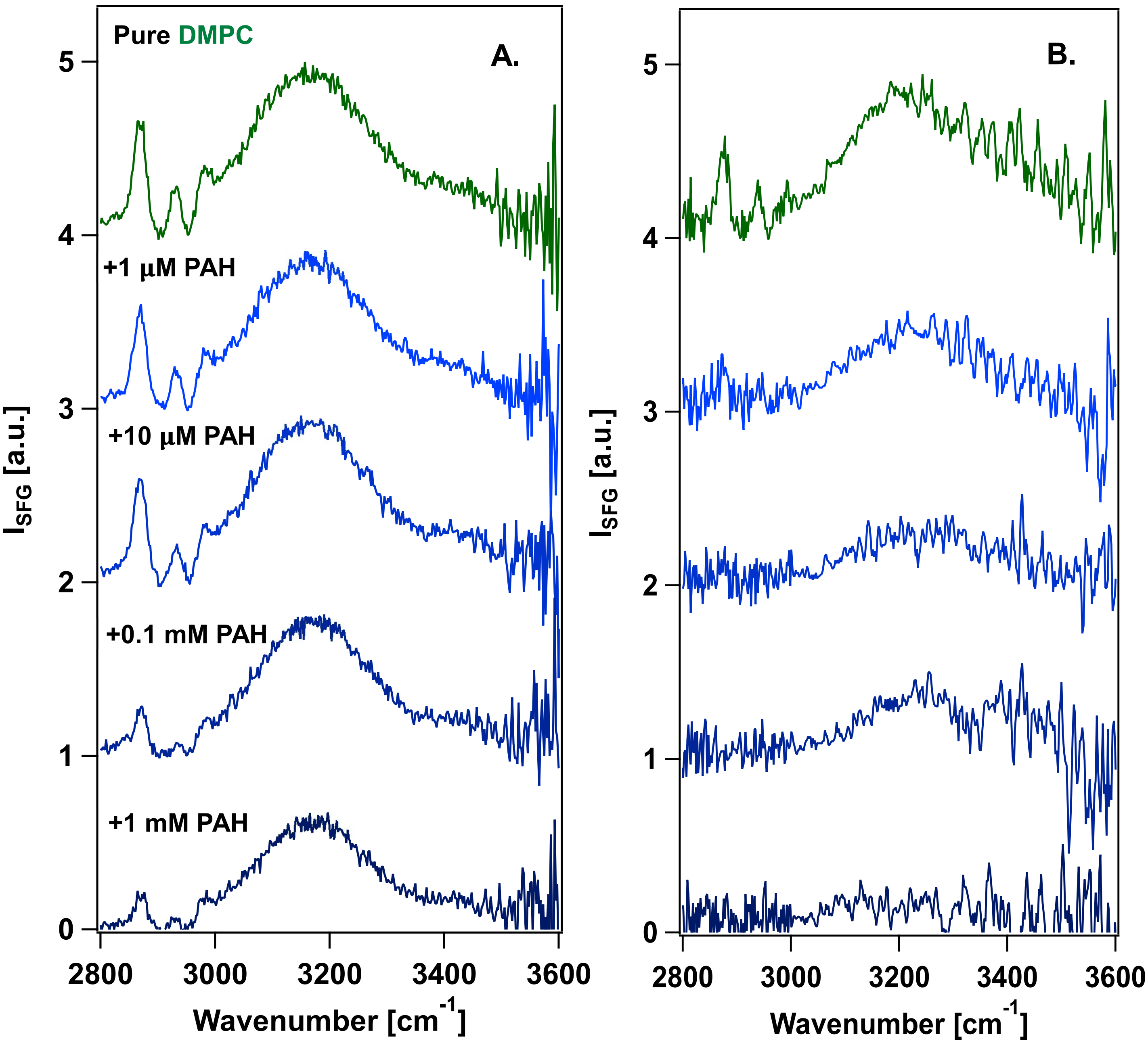

Major Response

Minor Response

Figure 3.

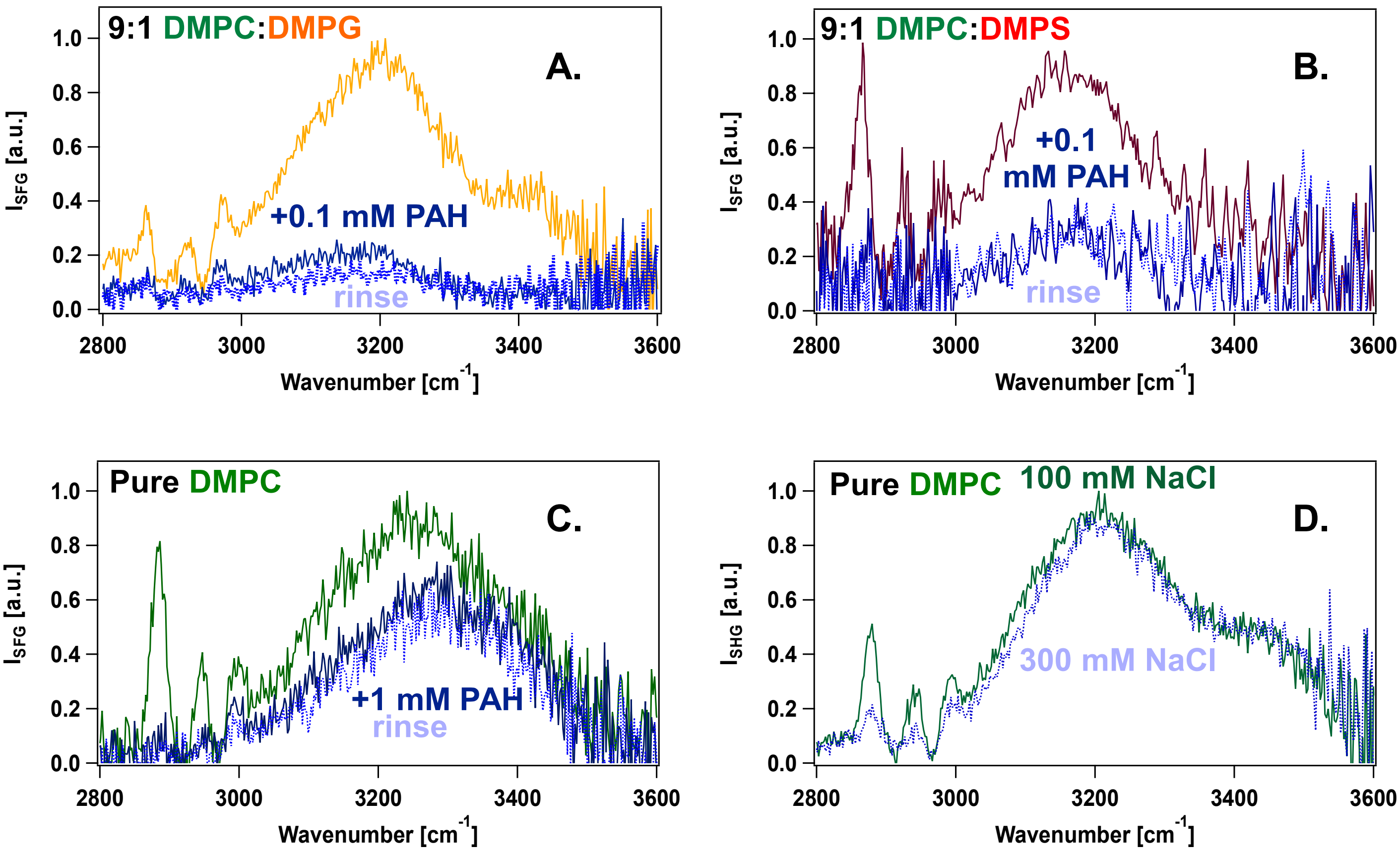

Figure 4.

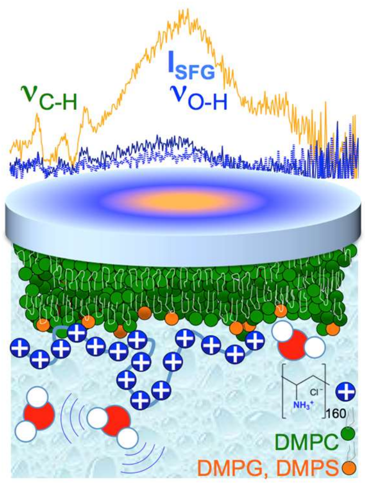

TOC Graphic